ANL-7740

Argonne National Laboratory

AN EXPERIMENTAL STUDY OF LOW-QUALITY, STEAM-WATER CRITICAL FLOW AT MODERATE PRESSURES

by

Robert E. Henry

Printed in the United States of America
Available from
National Technical Information Service
U.S. Department of Commerce
Springfield, Virginia 22151
Price: Printed Copy $3.00; Microfiche $0.65

ANL-7740
Reactor Technology

ARGONNE NATIONAL LABORATORY
9700 South Cass Avenue
Argonne, Illinois 60439

AN EXPERIMENTAL STUDY OF LOW-QUALITY, STEAM-WATER CRITICAL FLOW AT MODERATE PRESSURES

by

Robert E. Henry

Reactor Analysis and Safety Division

September 1970

TABLE OF CONTENTS

LIST OF FIGURES

LIST OF TABLES

NOMENCLATURE

G	Mass flow rate per unit area
H_0	Stagnation enthalpy
h	Enthalpy
k	Velocity ratio u_g/u_ℓ
P	Static pressure
s	Entropy
u	Velocity
v	Specific volume
x	Quality

Greek Letters

α	Void fraction
γ	Isentropic exponent
ρ	Density

Subscripts

c	Critical condition
E	Equilibrium
e	Exit plane
F	Frozen ($dx/dP = 0$)
g	Gaseous phase
H	Homogeneous ($u_g = u_\ell$)
ℓ	Liquid phase
R	Receiver
sat	Saturation
w	Wall

FOLD-OUT

AN EXPERIMENTAL STUDY OF LOW-QUALITY, STEAM-WATER CRITICAL FLOW AT MODERATE PRESSURES

by

Robert E. Henry

ABSTRACT

Data for two-phase, steam-water critical flow were obtained in a long, constant-area duct. The ranges of parameters studied were (1) flow rates from 1649 to 6603 $lb_m/sec\text{-}ft^2$, (2) exit pressures from 150 to 300 psia, and (3) thermodynamic-equilibrium qualities from 0.0030 to 0.1467. The data exhibit the same general trends as previously published low-pressure (40-150 psia) experimental results, and they are also in good agreement with a correlation derived from the low-pressure data.

I. INTRODUCTION

Safety analyses of pressurized boiling-water, and liquid-metal-cooled nuclear reactors require a knowledge of one-component, two-phase critical flow in the low-quality region where the assumption of thermodynamic equilibrium is questionable.[1] A considerable amount of experimental information has been accumulated for steam-water systems in the pressure range $P_e \leq 150$ psia, and this has been very useful in structuring critical-flow studies of sodium.

Typical operating pressures for pressurized and boiling-water reactors are from 2000 to 2200 psia. It is desirable to know if the results of the low-pressure studies are characteristic of such higher pressure levels. The objectives of this study were to:

(1) Obtain data for steam-water, two-phase, critical flow in the quality range $0.001 < x_{Ee} < 0.15$ for exit pressures ranging from 150 psia to the limit of the facility, which was 300 psia.

(2) Evaluate the reliability of various analytical and semiempirical models on the basis of the experimental data.

II. PREVIOUS WORK

Recent experimental studies of one-component, two-phase critical flows in long constant-area ducts are reviewed in Ref. 1. Most of these investigations[1-6] were restricted to exit pressures less than 150 psia and thus are comparable to the experimental data of Ref. 1. The investigations described in this chapter, with the exception of those in Ref. 1, are concerned with exit pressures greater than 150 psia.

Agostinelli and Salemann[7] presented a limited amount of data on the low-quality critical flow of steam-water mixtures through fine annular clearances. The exit pressures ranged from 200 to 300 psia; however, the only pressure tap in the vicinity of the exit plane was located in the downstream plenum. As discussed in Ref. 1, the meaning of such a measurement is difficult to evaluate for steam-water mixtures. It is virtually impossible to determine the actual exit pressure by this means.

Fauske[8] reported extensive data for steam-water critical flows in the quality range $0.01 \leq x_{Ee} \leq 0.70$ and for exit pressures in the range 40 psia $\leq P_e \leq$ 360 psia. The results were in good agreement with the slip-flow model he developed.

Zaloudek[9] investigated the high-pressure discharge of very low-quality mixtures. The operating ranges were 421 Btu/$lb_m \leq H_0 \leq$ 533 Btu/lb_m and 200 psia $\leq P_e <$ 800 psia. When the fluid entering the test section was in a two-phase condition, the experimental data showed good agreement with the Fauske model. When the incoming fluid was in a subcooled liquid state, the experimental flow rates were considerably greater than those predicted by the Fauske model.

Henry[1] experimentally investigated the low-quality discharge of steam-water mixtures in the quality range $0.0019 \leq x_{Ee} \leq 0.216$ and for exit pressures from 40 to 150 psia. In addition to the usual measurements of temperature, pressure, and flow rate, the local void fraction at the exit plane was measured by gamma-ray attenuation. The velocity ratios ($k = u_g/u_\ell$) obtained were far less than those predicted by the models of Fauske,[8] Levy,[10] Moody,[11] and Cruver.[5] Although these models yield relatively accurate predictions for the critical flow rates in the range $0.01 \leq x_{Ee} \leq 1.0$, they do not correctly describe the physical phenomena in the low-quality range examined by Henry.

The measured void fractions were used to correlate for the non-equilibrium processes of slip between the phases and a retarded phase change. This approach yielded a simple correlation for the critical flow which can be expressed as

$$G_c = G_{cHE}(20\, x_{Ee})^{-1/2}, \tag{1}$$

where G_{cHE} is the critical mass flow rate for Homogeneous Equilibrium Model (HEM), defined by

$$G_{cHE} = -\left(\frac{\partial P}{\partial v}\right)_s \tag{2}$$

and

$$v = (1 - x_E)\, v_\ell + x_E v_g; \tag{3}$$

$$s = (1 - x_E)\, s_\ell + x_E s_g. \tag{4}$$

(The thermodynamic properties are functions of the saturation pressure only and can be obtained from the Steam Tables.[12])

The experimental study of Ref. 1 illustrated the influence of the exit plane geometry on the measurements of wall pressure taps located in the immediate vicinity. Test sections with rapid expansions at the exit plane, such as those used by Fauske[8] and Zaloudek,[9] experience large two-dimensional effects in the neighborhood of the exit, as shown in Fig. 1. To evaluate the extent of this influence, a rapid expansion and a 7° included angle divergent exit geometries were studied. The test sections were operated under identical conditions, and the resulting mass flow rates are compared in Fig. 2. The discrepancies between the results are caused by

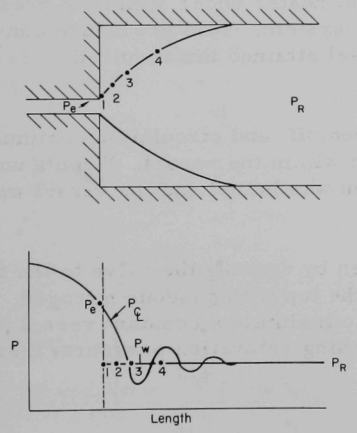

Fig. 1. Two-dimensional Aspects of a Rapid Expansion. ANL Neg. No. 112-9295.

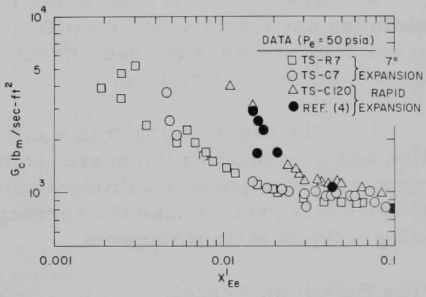

Fig. 2. Data Comparison for Different Downstream Geometries. ANL Neg. No. 112-9312 Rev. 2.

the two-dimensional expansion downstream. The 7° divergent geometry reduces the two-dimensional behavior at the throat so that a measurement recorded by a wall tap is more indicative of the centerline pressure where the choking phenomena actually occurs. Additional experimental verification of this behavior has been reported by Kelly[13] for low-pressure steam-water critical flow in a diabatic system.

III. EXPERIMENTAL APPARATUS

The experimental critical-flow data were obtained with an instrumented test section extending from the blowdown vessel as shown in the schematic diagram (Fig. 3) of the experimental apparatus. The operating procedure, test section, and major components, as well as basic measurement techniques, are described in this chapter. The experimental data are summarized in tabular form in the Appendix.

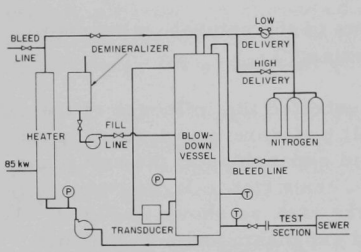

Fig. 3. Experimental Apparatus. ANL Neg. No. 112-9310.

A. Operating Procedure

The operating procedure was as follows:

1. The facility was filled with demineralized water at 70°F. The water was circulated through the 85-kW electrical heater under sufficient pressure to retain a liquid state throughout the system. This procedure continued until the water in the blowdown vessel attained the required (predetermined) temperature.

2. The electrical heater was turned off, and circulation continued to minimize any temperature stratification within the vessel. When a uniform temperature was obtained, circulation was halted and the vessel was isolated from the heating loop.

3. The experimental run was taken by opening the valve to the test section and pressurizing the vessel from the top with gaseous nitrogen. The nitrogen was supplied at a sufficient rate to maintain a constant vessel pressure which was greater than the corresponding saturation pressure, thereby insuring a liquid state throughout.

B. The Blowdown Vessel

The vessel was constructed from a 21-in.-ID steel cylinder, was 180 in. long with $2\frac{1}{2}$-in. walls. It can hold approximately 2000 lb of water and was hydrostatically tested to 2200 psi along with the rest of the basic apparatus.

C. Nitrogen System

The nitrogen system consisted of six nitrogen bottles and two delivery lines. The low-flow delivery system was governed by a Victor air regulator and was capable of maintaining the tank pressure to within ±1 psi. The high-flow delivery line was controlled by an air-operated, 1/2-in. Annin valve, which maintained the pressure to within ±2 psi.

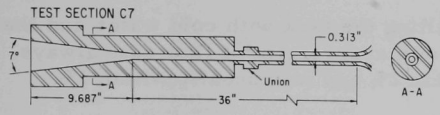

Fig. 4. Test Section. ANL Neg. No. 112-9309A.

D. Test Section

The test section used in this investigation (see Fig. 4) was 36 in. long and constructed of Type 304 stainless steel. There was no readily available method for making the section in one piece because of its length. Consequently, it had to be fabricated in two parts. The construction details are given in Ref. 1.

E. Pressure Measurement

Table I lists the locations of the pressure taps, their sizes, and the accuracy of measurement obtainable. All pressure measurements were obtained using Bourdon-tube pressure gauges, which were periodically calibrated against a dead-weight tester.

TABLE I. Pressure-tap Installations

Designation	Distance from Exit Plane, in.	Diameter of Tap, in.	Accuracy of Pressure Measurement, psi
U8	+30.0	1/16	±5
U7	+15.0	1/16	±5
U6	+6.0	1/16	±5
U5	+2.747	1/16	±5
U4	+1.498	0.010	±5
U3	+0.502	0.010	±2
U2	+0.032	0.010	±2
U1	+0.011	0.010	±2
t	+0.000	0.010	±2

F. Measurement of Flow Rate

Since the blowdown vessel was quite tall and the water in the tank was in a subcooled state, a convenient method for measuring the flow rate was to determine the time interval required for the static head in the vessel to decrease a given amount. The time interval was measured with a stopwatch and the head drop by a Statham ±5 psi differential pressure transducer,

which was connected to pressure taps located at the bottom and top of the tank (see Fig. 3). The input signal to the transducer was provided by a Hewlett-Packard power supply, and the output was read on a four-digit Hewlett-Packard digital voltmeter. The head of nitrogen above the water was taken into account by assuming the nitrogen was at the same temperature as the water; this did not produce more than a 1-2% correction in the flow rate.

This method was checked by filling the tank with cold water and then blowing it down into a weight tank. The measurement of flow rate always agreed with the weight-tank value within 2% and was usually within 1%.

The differential pressure transducer was calibrated with a mercury manometer before and after each run.

G. Temperature Measurement

Two thermocouples were used in the blowdown system. A chromel-alumel thermocouple was used in the tank, and an iron-constantan thermocouple was used in the 1/2-in. pipe leading to the test section. Both were calibrated in a silicone-oil bath using a platinum resistance thermometer as the standard. A Mueller bridge and a Leeds and Northrup galvanometer were used to determine the temperature of the platinum resistance thermometer, and the thermocouples were read on a Leeds and Northrup potentiometer.

During a test run, both thermocouples were recorded and an agreement of $\pm 0.5°F$ was attained.

H. Evaluation of Equilibrium Quality

The equilibrium quality at the exit plane was based on the homogeneous energy equation

$$H_0 = \left[(1 - x_E)\, h_\ell + x_E h_g\right]_e + \frac{G_c^2}{2}\left\{(1 - x_E)\, v_\ell + x_E v_g\right\}_e^2. \qquad (5)$$

(The subscript e indicates that all included quantities are evaluated at the exit plane.) The stagnation enthalpy was evaluated from the measured stagnation temperature, and the flow rate is the experimentally measured value; all properties are the equilibrium values associated with the measured exit pressure. This formulation was used so that the experimental results would be directly comparable with those of other studies.

IV. DISCUSSION OF RESULTS

A. Comparison between Data and Theoretical Models

The data for exit pressures of 150, 200, 250, and 300 psia are shown in Figs. 5, 6, 7, and 8 respectively. (All the experimental results and the accompanying axial pressure profiles are tabulated in the Appendix.) For

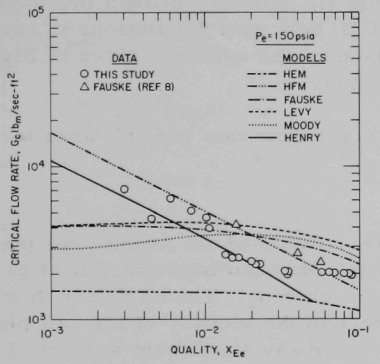

Fig. 5. Comparison between Analytical Models and Experimental Data for P_e = 150 psia. ANL Neg. No. 113-3488.

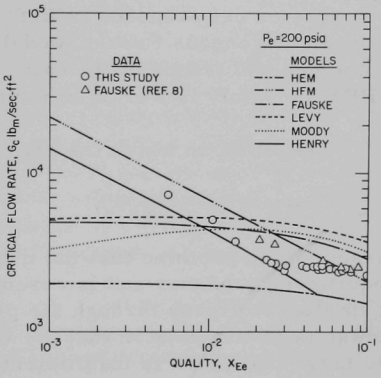

Fig. 6. Comparison between Analytical Models and Experimental Data for P_e = 200 psia. ANL Neg. No. 113-3486.

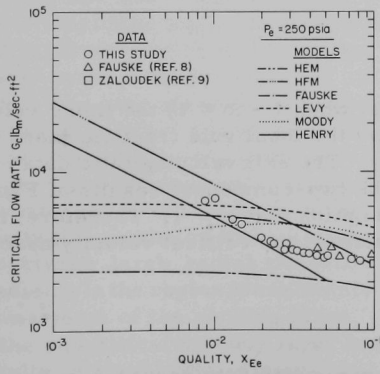

Fig. 7. Comparison between Analytical Models and Experimental Data for P_e = 250 psia. ANL Neg. No. 113-3489.

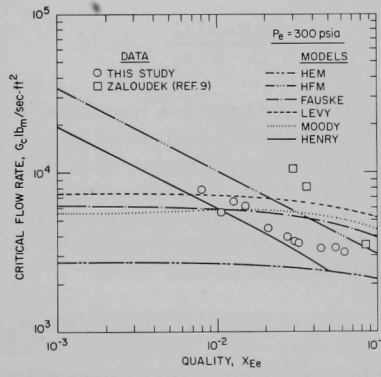

Fig. 8. Comparison between Analytical Models and Experimental Data for P_e = 300 psia. ANL Neg. No. 113-3487.

comparison the available data of Fauske[8] and Zaloudek[9] are also included along with predictions of several prominent theoretical models published in the literature. For all pressure levels studied, the models which assume thermodynamic equilibrium between the phases (Homogeneous Equilibrium, Fauske,[8] Levy,[10] and Moody[11]) do not agree with the experimental data in the low-quality region ($x_{Ee} < 0.05$). This observation is in agreement with the low-pressure results reported in Ref. 1.

The model proposed in Ref. 1 with its solution outlined in Chapter II and the Homogeneous Frozen Model (HFM) both give predictions in accord with the general trends of the data. Based on the evidence given in Figs. 5-8, the HFM certainly is worthy of further study.

The HFM, in which the critical mass flow rate per unit area is

$$G_{cHF} = \gamma P_e / x_{Ee} v_g, \tag{6}$$

is based on the premise that the mixture expands to the throat (exit plane) in an equilibrium manner and is essentially frozen (no interphase heat or mass transfer) as it passes through the plane of choking. The basis for this premise is an assumption that the velocity in the vicinity of the exit plane is so large that there is insufficient time for any significant amount of mass transfer to occur.

As part of the experimental low-pressure study described in Ref. 1, the average void fraction at the throat was measured with a one-shot gamma-ray-attenuation technique. The one-dimensional liquid-continuity equation can be written as

$$u_\ell = \frac{(1 - x)\, G}{(1 - \alpha)\, \rho_\ell}. \tag{7}$$

Therefore, at very low qualities (that is, when $1 - x \approx 1$) the liquid velocity can be accurately estimated if one knows the local void fraction, mass flow rate, and the approximate liquid density. The exit velocity ratio data reported in Ref. 1, when compared to the two-component results of Fauske,[14] give credence to the homogeneous assumption that $k = 1$. Therefore, if the flow is indeed "frozen" as the HFM assumes, the critical velocity associated with the HFM:

$$u_c = G_{cHF}[(1 - x_E)\, v_\ell + x_E v_g]_e, \tag{8}$$

should exhibit good agreement with the measurements reported in Ref. 1. The predictions of critical velocity of the HFM and HEM are compared with the experimental data in Fig. 9. It is readily apparent that the data are in closer agreement with predictions of HEM than with those of HFM.

Therefore, the comparatively good prediction of flow rate by the HFM is due to a compensating effect between the velocity and the mixture specific volume. Thus, the HFM does not correctly describe the physical phenomenon.

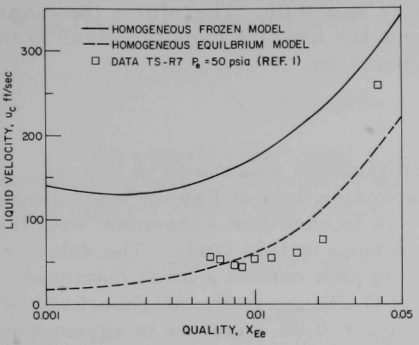

Fig. 9. Comparison of Measured Critical Velocities with the Homogeneous Models. ANL Neg. No. 900-5 Rev. 1.

In reality, the quality for these flows is something less than the equilibrium value, and the rates of interphase heat and mass transfer at the throat lie somewhere between the limiting equilibrium and frozen models. The formulation presented in Ref. 1, although it loses some realism in the experimental correlation, is superior to the equilibrium and frozen approaches because it attempts to treat the real phenomena described above.

The prediction for dimensionless critical flow rate developed in Ref. 1 is compared to the low-quality data in Fig. 10. The model and the experimental results are in good agreement for all the exit pressure levels studied herein.

B. Geometrical Comparisons

Figures 5-8 and 10 show that the data discrepancies between the 7° included angle divergence and rapid-expansion test sections, which were initially reported in Ref. 1, are also apparent at higher pressure levels. These discrepancies are due to the differences in the two-dimensional behavior downstream of the choking plane. The rapid-expansion test sections experience large radial pressure gradients in the region immediately downstream of the choking plane. The effect of this expansion is also felt in the subcritical viscous layer immediately upstream of the exit. This results in sizable two-dimensional pressure gradients such that a wall pressure tap located in this region does not record a measurement characteristic of the free stream where the choking phenomenon occurs. The 7° divergence geometry greatly reduces the magnitude of the two-dimensional expansion and, thus, a wall-pressure measurement in the vicinity of the exit plane is more characteristic of the free-stream value. Based on these

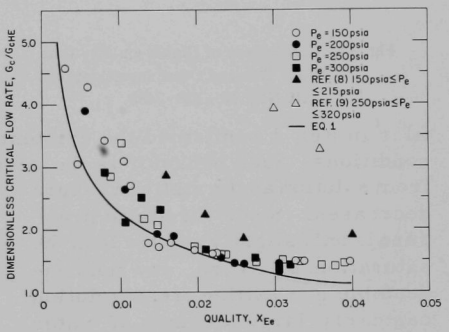

Fig. 10. Comparison of Henry's Correlation and Experimental Data for All Pressure Levels. ANL Neg. No. 113-3484.

observations, the data taken with the 7° divergence geometry are considered to be more representative of the critical-flow phenomenon. It should be noted that the discrepancies are considerable in the low-quality region and essentially disappear for qualities greater than 0.06. Therefore, the magnitude of the differences is dependent upon the mixture density, which is in agreement with the two-dimensional explanation.

C. General Observations

The experimental data for higher qualities are shown in Fig. 11. For qualities greater than 0.06, the rapid-expansion data of Fauske[8] and Zaloudek[9] are in excellent agreement with the results of this study. The data for 150 psia exhibit a local maximum of G_c/G_{cHE} in the neighborhood of $x_{Ee} = 0.08$, which is in agreement with the low-pressure findings.[1]

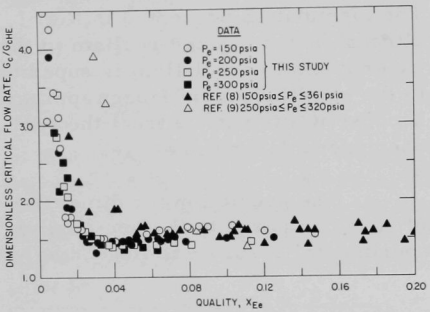

Fig. 11. Comparison of Higher-quality Data from This and Other Investigations. ANL Neg. No. 113-3483.

Figure 12 displays the axial pressure profile for Run No. 31. The gradient deviates from the constant value characteristic of incompressible flow before the saturation pressure is reached. This deviation is indicative of acceleration which can only be accomplished by the formation of a compressible (gaseous) phase. The axial void-fraction profiles in Ref. 1 confirmed the existence of a gaseous phase under similar conditions. Such behavior is the result of previously dissolved gases exiting from solution as the static pressure decreases. Since the static pressure is only slightly greater than the saturation pressure, any noncondensible gas exiting from solution can carry large amounts of water vapor in the form of humidity and, thus, act as a source for vapor formation prior to reaching saturation.

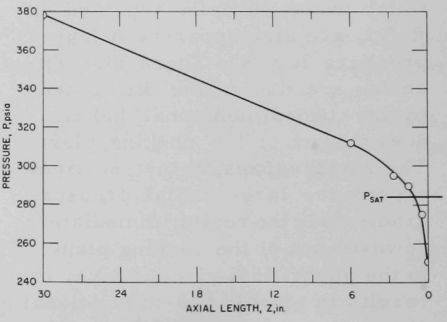

Fig. 12. Axial Pressure Profile for Run No. 31. ANL Neg. No. 113-3485.

The oscillatory behavior at low qualities which was reported by several previous investigators[4-6] was not observed by Henry[1] or in this work. As discussed in Ref. 1, in the studies in which such oscillations were observed, superheated steam and subcooled water were mixed to obtain the desired stagnation conditions. For low-quality flows, the net stagnation condition may be

saturated or subcooled water, in which case all the steam is condensed and the system should experience water-hammer effects. It is believed that the observed pressure oscillations are due to these effects and not to "slug flow" as suggested in Refs. 4-6.

V. SUMMARY AND CONCLUSIONS

An experimental study was undertaken to obtain detailed data on the low-quality critical flow of one-component, two-phase mixtures for moderately high pressures (150 psia $\leq P_e \leq$ 300 psia).

The major conclusions of this investigation can be stated as follows:

(1) The low-quality data exhibit good agreement with the non-equilibrium model presented in Ref. 1.

(2) The high-pressure, low-quality results show discrepancies between the 7° included angle divergence and rapid-expansion test sections similar to those witnessed at lower exit pressures. The results of the 7° divergent test section are more representative of the actual two-phase critical-flow phenomenon.

APPENDIX

Data Tabulation

TABLE II. Critical Flow Data

Run	H_0, Btu/lb_m	G_c, lb_m/sec-ft^2	Exit Parameters P_e, psia	Exit Parameters x_{Ee}	G_c/G_{cHE}
1	334.2	4570	149	0.0045	3.05
2	340.6	3952	149	0.0113	2.70
3	332.1	6247	142	0.0059	4.27
4	332.1	7114	147	0.0030	4.57
5	338.5	5178	150	0.0081	3.43
6	340.6	4637	150	0.0105	3.10
7	347.0	2394	148	0.0196	1.64
8	350.2	2299	149	0.0225	1.63
9	350.2	2309	150	0.0219	1.60
10	358.8	2071	148	0.0326	1.49
11	360.9	2068	150	0.0338	1.49
12	366.3	2003	150	0.0397	1.47
13	383.6	2037	152	0.0569	1.57
14	395.6	2013	153	0.0690	1.61
15	369.5	3538	198	0.0169	1.90
16	365.2	5112	200	0.0106	2.64
17	358.8	7330	195	0.0055	3.90
18	368.4	3669	200	0.0147	1.92
19	377.1	2690	200	0.0248	1.46
20	378.2	2690	200	0.0260	1.46
21	381.4	2409	199	0.0304	1.32
22	397.8	2463	199	0.0485	1.42
23	390.2	2590	201	0.0390	1.47
24	388.0	4630	247	0.0148	2.07
25	397.8	2539	201	0.0474	1.48
26	396.7	3528	251	0.0235	1.60
27	397.8	2497	203	0.0466	1.45
28	396.7	3551	252	0.0231	1.61
29	376.0	2849	201	0.0230	1.54
30	382.5	2615	201	0.0305	1.45
31	388.0	4970	251	0.0130	2.19
32	407.7	3050	251	0.0364	1.43
33	403.3	2479	204	0.0522	1.46
34	384.7	6532	251	0.0088	2.84
35	408.8	2981	251	0.0377	1.41
36	412.2	2455	201	0.0632	1.49
37	405.5	1989	151	0.0802	1.62
38	386.9	7776	252	0.0102	3.39
39	393.4	3820	251	0.0196	1.71

TABLE II (Contd.)

Run	H_0, Btu/lb_m	G_c, lb_m/sec-ft^2	Exit Parameters P_e, psia	x_{Ee}	G_c/G_{cHE}
40	391.2	2550	200	0.0407	1.45
41	389.1	2042	150	0.0636	1.61
42	475.9	2620	250	0.1128	1.47
43	471.3	2178	205	0.1253	1.50
44	469.0	1649	151	0.1467	1.55
45	420.0	3708	301	0.0305	1.46
46	416.6	2868	246	0.0487	1.41
47	414.4	2424	203	0.0648	1.47
48	411.1	2004	152	0.0853	1.66
49	402.2	5615	297	0.0106	2.13
50	398.9	3215	248	0.0275	1.49
51	394.5	2573	199	0.0447	1.47
52	401.1	7776	299	0.0080	2.92
53	412.2	4395	301	0.0210	1.69
54	410.0	3053	251	0.0389	1.45
55	407.7	2500	201	0.0583	1.50
56	403.3	1993	148	0.0794	1.64
57	432.3	3349	302	0.0447	1.36
58	430.1	2800	250	0.0622	1.41
59	425.6	2330	200	0.0783	1.46
60	424.4	1862	145	0.1027	1.66
61	407.7	6151	301	0.0151	2.32
62	404.4	3156	250	0.0330	1.48
63	401.1	2553	200	0.0515	1.50
64	441.4	3340	302	0.0551	1.39
65	439.1	2808	250	0.0721	1.45
66	422.2	3627	304	0.0320	1.43
67	420.0	2903	251	0.0504	1.42
68	416.6	2423	200	0.0685	1.48
69	413.3	1945	148	0.0897	1.65
70	448.2	3152	304	0.0625	1.34
71	447.0	2720	251	0.0808	1.42
72	447.0	2273	201	0.1008	1.50
73	441.4	1754	147	0.1196	1.59
74	404.4	6603	297	0.0127	2.52
75	402.2	3218	248	0.0312	1.51
76	344.9	2558	149	0.0166	1.78
77	341.7	2653	148	0.0136	1.78
78	417.7	3933	302	0.0274	1.53
79	414.4	2972	251	0.0440	1.43
80	420.0	2458	200	0.0719	1.52
81	408.8	1997	147	0.0853	1.67
82	342.7	2532	148	0.0149	1.70
82	342.7				
82	342.7				
82	342.7				
83	342.7				

TABLE III. Axial Pressure Profiles (psia)

Run	Position								
	8	7	6	5	4	3	2	1	Exit
1	222	194	179	173	171	165	153	150	149
2	210	199	177	173	170	163	152	149	149
3	251	198	171	163	160	155	144	142	142
4	257	205	178	170	167	162	151	149	147
5	232	197	179	173	171	165	153	150	150
6	221	194	179	173	172	165	153	150	150
7	196	187	179	173	169	161	151	149	148
8	202	194	184	177	173	164	152	149	149
9	208	197	187	180	175	165	154	150	150
10	215	205	195	185	179	168	152	149	148
11	219	210	200	189	182	168	152	150	150
12	242	231	212	195	187	171	155	150	150
13	255	236	210	200	190	174	156	152	152
14	289	264	230	207	193	176	158	154	153
15	267	250	238	230	226	215	202	199	198
16	293	261	242	234	230	221	204	201	200
17	352	280	244	232	227	218	201	196	195
18	270	253	240	231	227	217	203	200	200
19	272	262	250	239	234	222	204	200	200
20	272	261	250	239	232	221	204	200	200
21	283	270	255	244	237	222	203	199	199
22	322	302	278	256	246	227	204	199	199
23	302	288	270	253	247	229	206	203	201
24	355	321	302	288	280	270	252	247	247
25	320	303	281	261	247	230	206	201	201
26	347	-[a]	308	292	288	274	256	251	251
27	318	303	282	260	250	231	208	204	203
28	340	-	306	292	288	273	255	252	252
29	266	255	245	235	230	220	205	201	201
30	282	270	256	243	238	224	205	201	201
31	378	-	312	295	290	275	256	251	251
32	358	-	322	305	299	280	256	251	251
33	337	317	287	264	253	232	209	204	204
34	412	-	317	300	295	280	257	251	251
35	369	-	-	310	301	282	257	251	251
36	346	322	290	265	251	231	207	201	201
37	308	275	236	211	195	175	154	151	151
38	432	-	309	295	293	283	259	252	252
39	348	325	305	291	287	273	256	251	251
40	310	293	282	255	247	228	206	200	200
41	282	259	229	206	192	172	155	151	150

[a]Static pressure is greater than the maximum value for the gauge.

TABLE III (Contd.)

Run	Position								
	8	7	6	5	4	3	2	1	Exit
42	-	-	-	-	322	294	259	251	250
43	-	-	320	286	266	239	212	205	205
44	372	296	246	217	193	177	154	151	151
45	417	398	380	362	352	331	307	301	301
46	389	372	343	320	304	281	254	246	246
47	362	337	300	274	256	234	209	203	203
48	317	284	242	217	197	178	159	153	152
49	446	405	373	356	346	331	305	297	297
50	367	347	322	307	293	277	254	248	248
51	331	312	282	265	246	227	204	199	199
52	494	412	368	354	350	-	307	299	299
53	434	405	376	357	347	-	309	301	301
54	384	364	337	319	303	285	259	251	251
55	352	332	296	274	252	231	207	201	201
56	305	277	237	213	192	185	154	148	148
57	449	435	405	385	371	-	310	303	302
58	425	402	360	330	313	288	258	250	250
59	387	352	304	280	256	232	206	200	200
60	320	285	240	212	190	172	151	145	145
61	448	405	375	362	353	-	309	301	301
62	368	352	325	310	296	279	256	250	250
63	336	317	288	267	248	229	205	200	200
64	489	467	430	399	378	-	310	303	302
65	454	417	369	337	316	290	259	250	250
66	425	407	385	364	356	-	311	304	304
67	401	382	352	327	309	296	258	251	251
68	369	332	299	275	251	229	205	200	200
69	315	282	242	217	193	175	156	149	148
70	519	487	435	394	371	-	312	304	304
71	474	432	376	341	319	291	259	251	251
72	413	367	312	280	257	232	208	201	201
73	330	292	245	217	192	175	153	147	147
74	459	405	370	357	349	-	305	297	297
75	365	347	322	307	293	277	254	248	248
76	193	187	179	171	165	160	151	149	149
77	193	187	178	170	165	159	149	148	148
78	408	392	375	357	346	-	208	302	302
79	384	370	344	323	305	283	255	251	251
80	355	332	294	272	248	229	203	200	200
81	309	277	237	212	189	172	152	147	147
82	206	195	181	172	167	160	150	148	148

ACKNOWLEDGMENTS

I wish to thank Elmer Gunchin, who aided in the construction, maintenance, and operation of the experimental apparatus.

REFERENCES

1. R. E. Henry, *A Study of One- and Two-component Two-phase Critical Flows at Low Qualities*, ANL-7430 (Mar 1968).

2. H. S. Isbin, J. E. Moy, and A. J. R. Cruz, *Two-Phase Steam-Water Critical Flow*, AIChE J. *3*, 361 (1957).

3. D. W. Faletti and R. W. Moulton, *Two-Phase Critical Flow of Steam-Water Mixtures*, AIChE J. *9*, 247 (1963).

4. F. R. Zaloudek, *The Low Pressure Critical Discharge of Steam-Water Mixtures from Pipes*, HW-68936 (1961).

5. J. E. Cruver, *Metastable Critical Flow of Steam-Water Mixtures*, PhD thesis, University of Washington (1963).

6. W. J. Klingebiel, *Critical Flow Slip Ratios of Steam-Water Mixtures*, PhD thesis, University of Washington (1964).

7. A. Agostinelli and W. Salemann, *Prediction of Flashing Water Flow Through Fine Annular Clearances*, Trans. ASME, 1138 (1958).

8. H. K. Fauske, *A Contribution to the Theory of Two-phase, One-component Critical Flow*, ANL-6633 (Oct 1962).

9. F. R. Zaloudek, *Steam-Water Critical Flow from High Pressure Systems. Interim Report*, HW-80535 (Jan 1964).

10. S. Levy, *Prediction of Two-Phase Critical Flow Rate*, Trans. ASME, J. Heat Transfer, *87-C*, 53 (1965).

11. F. J. Moody, *Maximum Flow Rate of a Single Component Two-Phase Mixture*, Trans. ASME, J. Heat Transfer, *87-C*, 134 (1965).

12. J. H. Keenan and F. G. Keyes, *Thermodynamic Properties of Steam*, John Wiley & Sons, New York (1936).

13. J. T. Kelly, *Two-Phase Critical Flow*, M.S. thesis, Dept. of Nucl. Engr., MIT (Jan 1968).

14. H. K. Fauske, "Two-Phase and Two-and-One-Component Critical Flow," *Proc. of Symp. on Two-Phase Flow*, University of Exeter, Devon, England, *3*, S6101 (1965).